LA-UR-17-24403
Approved for public release; distribution is unlimited.

Title:	Testing and simulation of thermal and mechanical properties of additively manufactured parts using fused deposition modelling (FDM)
Author(s):	Baker, Andrew M. McCoy, John Majumdar, Bjaskar S. Rumley-Ouellette, Brittany Joy Wahry, Jacob Marchi, Alexandria Nicole Bernardin, John David Spernjak, Dusan
Intended for:	International Workshop on Structural Health Monitoring, 2017-09-12/2017-09-14 (Stanford, California, United States)
Issued:	2018-07-31 (rev.1)

Measurement and Modelling of Thermal and Mechanical Anisotropy of Parts Additively Manufactured Using Fused Deposition Modelling (FDM)

ANDREW M. BAKER[a], JOHN MCCOY[b],
BHASKAR S. MAJUMDAR[b],
BRITTANY RUMLEY-OUELLETTE[a],
JACOB WAHRY[a], ALEXANDRIA N. MARCHI[a],
JOHN D. BERNARDIN[a] and DUSAN SPERNJAK[a]

[a]Los Alamos National Laboratory, Los Alamos, NM 87545, U.S.A
[b]New Mexico Institute of Mining and Technology, Socorro, NM 87801, U.S.A

ABSTRACT

Fused deposition modelling (FDM) is an additive manufacturing (AM) technique which involves melting a thermoplastic filament material and subsequently extruding it, layer by layer, to create three-dimensional objects. The nature of this build process yields parts with inhomogeneous compositions, which may result in anisotropic thermal and mechanical properties. In this work, such anisotropies were investigated for different commercially-available FDM materials such as polylactic acid, acrylonitrile butadiene styrene, and polyurethane.

Due to the biaxial symmetry of some properties of resulting FDM parts, a transversely isotropic material model was developed for simulating the FDM part response to thermal and mechanical loads. Such a model is more robust than an isotropic model and, when compared to a full orthotropic model, requires fewer elastic constants to be experimentally determined. Ultimately, the development of FDM-specific thermomechanical property data and models for AM parts will provide more accurate parameters for part designs, leading to higher confidence in part qualification.

INTRODUCTION

Fused deposition modelling (FDM), a common method of 3-D printing, is an additive manufacturing (AM) technique for rapidly prototyping parts with custom geometries. Recently, there has been interest in modelling the thermomechanical load response of AM parts, such as those with embedded temperature and strain sensors for *in situ* structural health monitoring [1-3].

In order to design and manufacture compliant parts, it is necessary to understand how the properties of the precursor FDM filament materials translate to those of the finalized parts fabricated using FDM. While the FDM process, itself, has been extensively modelled [4], the effects of this process on the final properties of FDM parts are currently unclear. In addition, due to the inherent inhomogeneity of parts fabricated using FDM, measuring the resulting part properties and modelling their subsequent thermomechanical load response is not trivial.

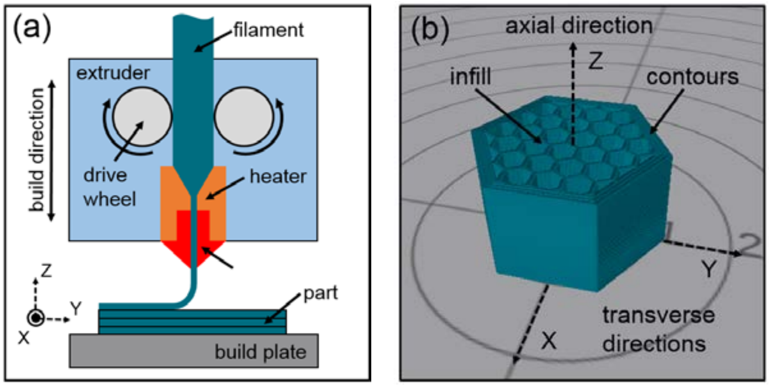

Figure 1. (a) A schematic of the FDM process and (b) an illustration of the layered construction of an FDM part, showing the non-uniform composition in the axial and transverse directions.

As shown in Figure 1a, during the FDM process, thermoplastic filament material is extruded through a heated nozzle to build up parts layer by layer in the XY plane. Initially, the filament is a bulk material with isotropic properties, however, its extrusion via FDM generates inhomogeneous parts. As shown in Figure 1b, part properties may differ in (i) the build direction (Z axis), called the "axial" direction and (ii) in the directions normal to the build direction, called the "transverse" directions (X and Y axes). For example, tensile properties between laminae in the axial direction will be different than those in transverse direction because of the continuity of the filament in the latter case. Bagsik showed that acrylonitrile butadiene styrene (ABS) tensile specimens are more ductile and have greater strain to failure in the transverse direction compared to the axial direction [5].

As shown in Figure 1b, FDM parts are enclosed by one or more boundaries in the XY plane, called "contours." The quantities of contours add further complexity to the thermomechanical part response. Bagsik showed that ABS tensile specimens printed in the XZ-plane (called "edge" orientation) contain more contours in the tensile direction compared to those printed in the XY-plane (i.e., transverse or "flat" orientation), which results in a 12% increase in strength [5]. Bhate also demonstrated that one or two contours result in similar tensile properties between parts, but adding between 5 and 10 contours to the part increases the strength and stiffness by over 10% [6].

The interior of the part consists of the "infill" (Figure 1b), which provides structural support to the outer contours. Infill pattern and density, along with infill penetration into the contours, as described by Bagsik in detail [7], may be specified by the part designer and will also affect the resulting thermal and mechanical part properties.

Besides contour count and infill characteristics, part properties may be influenced by other FDM print parameters such as layer height, print speed, and nozzle/print bed temperatures. Because these parameters can be unique for each FDM part, the combined effects of multiple fabrication parameters will add further complexity to the material model. While a full parametric investigation of these properties is beyond the scope of this study, OptiMatter has reported a large number of properties and trends for FDM parts printed with many commercially available filament materials [8].

Andrew M. Baker[a], John McCoy[b], Bhaskar S. Majumdar[b], Brittany Rumley-Ouellette[a], Jacob Wahry[a], Alexandria N. Marchi[a], John D. Bernardin[a], Dusan Sperjnak[a]
[a.] Los Alamos National Laboratory, Los Alamos, NM 87545, U.S.A
[b.] New Mexico Institute of Mining and Technology, Socorro, NM 87801, U.S.A

In addition to many of the FDM print parameters, the anisotropic nature of parts fabricated via FDM is not always well reported. Such anisotropy is important to consider because it could have a strong effect on the thermomechanical response of FDM parts. For example, the average tensile modulus of ABS FDM parts reported in the literature is ~2.0 GPa [9, 10]. This value is nearly identical to the values for parts fabricated in both axial and transverse orientations using commercial FDM machines [11]. The literature average maximum stress of FDM ABS parts is ~33 MPa [9, 10]. Comparing this value to those for commercial FDM ABS parts, this value is identical to the transversely fabricated specimen, however it is over 20% larger than the axial specimen [11].

In addition to tensile properties, compressive and thermal properties are even more sparsely reported for ABS and other materials such as polylactic acid (PLA) and polyurethane (PU), and reported values vary between sources [5, 9, 12]. As a result, it is currently unclear how to implement these material properties into a model for thermomechanical simulation. Depending on the required accuracy of the material model, this anisotropy could have a significant effect on the predicted part response.

Due to the sparse reporting of anisotropic properties in the literature, this paper supplements and extends the available literature data with additional testing of compressive properties, coefficient of thermal expansion (CTE), glass transition temperature (T_g), and heat capacity (C_p) in both the axial and transverse directions for FDM parts composed of PLA, ABS, PU and conductive PLA.

To illustrate the effects of measured anisotropy on the tensile response of FDM parts, we employ a transversely isotropic mechanical model. Such a method will allow for accurate simulation of part response with fewer required mechanical tests compared to a fully orthotropic material model.

EXPERIMENTAL METHODS

Materials and FDM print parameters

All specimens were printed using a Rostock MAX V2 3-D printer with a 0.5 mm diameter brass nozzle. The printer was controlled from G-code generated using MatterControl 1.5 software. All parts were printed without any contours, using 100% infill density with a linear infill pattern (called "lines" in software notation), which was previously shown to maximize tensile properties [8]. Layer height and nozzle travel velocity were kept constant at 0.2 mm and 40 mm/s, respectively. Using these parameters, the filament extrusion rate provided by the drive wheel was automatically calculated by the control software. Nozzle (T_{nozzle}) and bed (T_{bed}) temperatures were determined by manufacturer specifications and were kept constant throughout the duration of the print (Table I).

Four commercially-available FDM filament materials were used: (1) PLA, (2) ABS, (3) PU and (4) electronically-conductive PLA (C-PLA). Material information and print parameters are summarized in Table I. Prior to FDM printing, filaments were desiccated for over 24 hours at <10% RH to reduce any moisture effects.

TABLE I. PRINT SPECIFICATIONS OF THE FDM FILAMENT MATERIALS TESTED.

Material	Manufacturer	T_{nozzle} (°C)	T_{bed} (°C)
PLA	MatterHackers Pro Series PLA	210	60
ABS	MatterHackers Pro Series ABS	228	80
PU	FennerDrives SemiFlex	228	80
C-PLA	ProtoPasta Conductive PLA	210	60

Compression testing

Compression testing was performed on FDM cylinders which were 2.54 cm high and 1.27 cm in diameter cylinders using an Instron 1125 R5500 load frame. Strain rate was 0.254 mm/min, and strain was continuously measured using an extensometer. Poisson's ratio was measured using a strain gage. Stresses are reported as "engineering" values, calculated as the force divided by the initial cross sectional area. Conversion to "true" stresses will result in noticeable differences at high strains [13].

Elastic modulus was calculated from the initial slope after the startup toe, which is a typical instrumentation error due in part to machine compliance and in part to inconstancy in the FDM samples. Yield stresses and strains were calculated at the peak where stress levels off. Maximum stress was also measured during testing and strain to failure was taken as the maximum strain measured at part failure.

Glass transition temperature and specific heat

T_g and C_p were measured on 10-15 mg FDM samples using a differential scanning calorimeter (TA Instruments Q2000). Heating/cooling rate of 10°C/min for PLA, ABS and PU, and 5°C/min for and C-PLA from -5°C to 280°C. T_g was calculated from the first dip in the heat flow response. Due to ambiguity of the heating curves typical of physical aging, T_g was calculated from the cooling curves following an initial heating to roughly 10°C above the glass transition. C_p was calculated by dividing the measured heat flux in the glassy phase by the heating rate.

Coefficient of thermal expansion

CTE measurements were performed on FDM cylinders which were 2 cm long and 0.65 cm in diameter, using a Linseis dilatometer. Heating was applied at a nominal rate of 2°C/min from room temperature to 100°C. In order to account for possible material phase transitions before and after the T_g, CTE coefficients were obtained by performing a linear regression on the 20°C and 80°C regions of the expansion curves.

RESULTS

Compressive properties

Compressive properties for PLA, ABS, PU (when available), and C-PLA in the axial and transverse directions are shown in Figure 2 through Figure 4. These values were calculated from the raw compression test data reported in Reference 14.

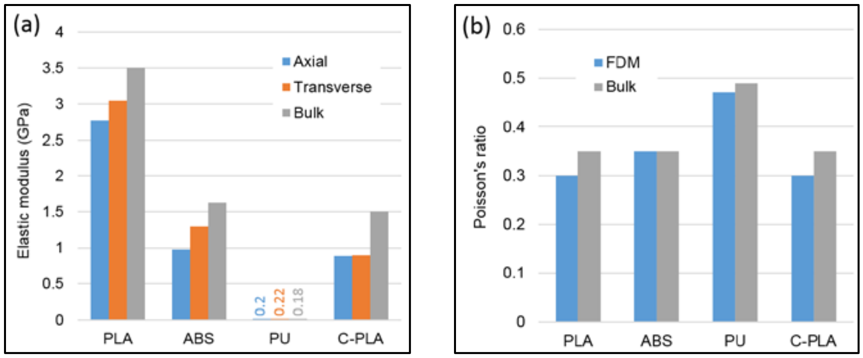

Figure 2. Compressive (a) moduli, (b) Poisson's ratios for PLA, ABS, PU, and C-PLA.

From Figure 2a, we observe that for FDM PLA, PU and C-PLA parts, axial and transverse moduli differed by less than 10%. Depending on the required accuracy of a material model, the moduli for FDM PLA, C-PLA and PU parts may be taken as isotropic. For ABS, however, the transverse modulus was more than 25% larger than the axial modulus, and thus, an isotropic stiffness model is not recommended. For PLA, ABS, and C-PLA, there was also deviation of their moduli from the bulk value. The PU modulus, however, was equivalent to the bulk value. Therefore, in general, using the bulk compressive modulus value for a new material is not recommended.

Poisson's ratio results are shown in Figure 2b. Here, the values were identical in both the axial and transverse directions. Values for ABS and PU were less than 5% from bulk values, however bulk values were more than 14% larger for both PLA and C-PLA, but these deviations are likely within the error of the measurement. Therefore, using a bulk, isotropic Poisson's ratio input for a new material may be used within an uncertainty of ±0.05.

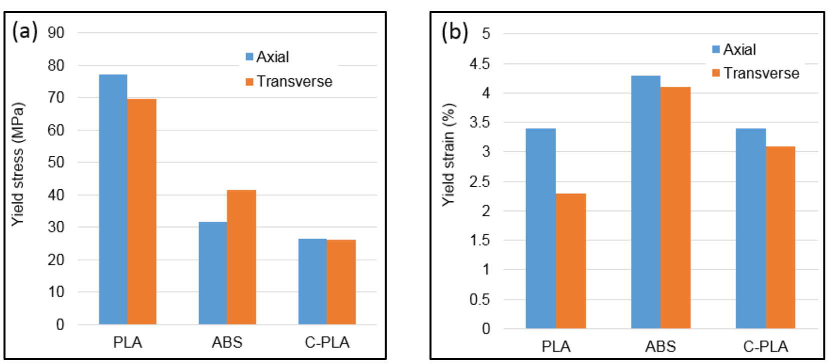

Figure 3. Compressive (a) yield stress and (b) yield strain for PLA, ABS, and C-PLA.

Compressive yield stress and strain are reported in Figure 3a and Figure 3b, respectively. Due to the elastomeric response of PU, the strain limit on the load frame was exceeded before it yielded, so yield properties were not determined. In FDM PLA and C-PLA parts, axial and transverse yield stresses differed by less than 10%, allowing for reasonable isotropic assumptions. For ABS, yield stress was over 23% larger in the transverse direction, and thus, an anisotropic yield stress model is suggested. Yield strain showed different behavior than yield stress and modulus. Here, the yield strains of ABS and C-PLA could be assumed isotropic (less than 10% deviation, each), while yield stress for PLA was over 32% greater in the axial direction.

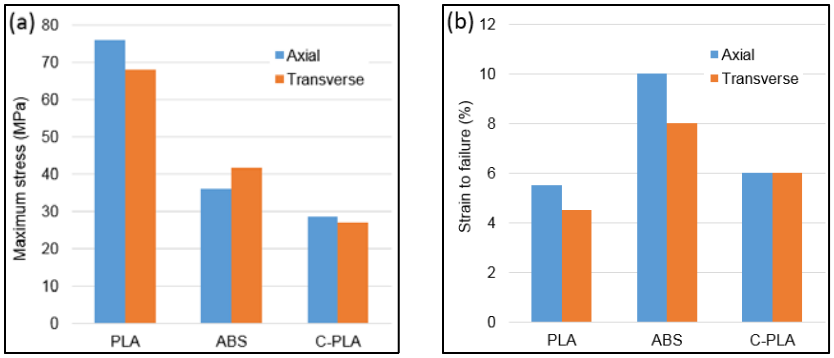

Figure 4. (a) Max. compressive stress and (b) compressive strain to failure for PLA, ABS, and C-PLA.

Maximum stress and strain to failure are shown in Figure 4a and Figure 4b, respectively. Here, the axial and transverse (or, through-plane and in-plane) quantities differ by more than 10% between the axial and transverse directions for PLA and ABS, which indicates that anisotropic maximum stress and strain to failure models are recommended. For C-PLA, maximum stress and strain to failure could be assumed to be isotropic.

Thermal properties

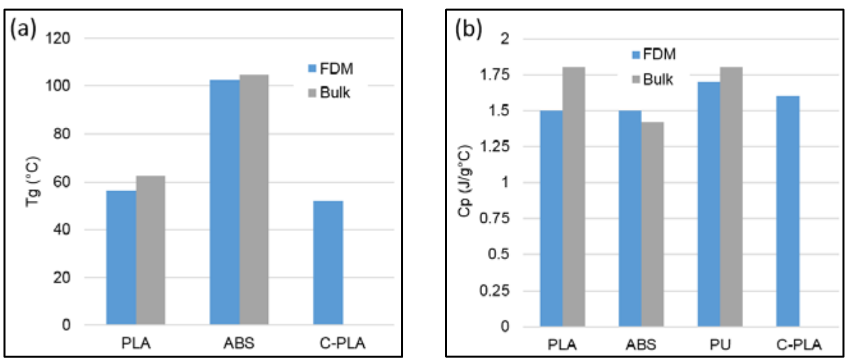

Figure 5. (a) Glass transition temperature and (b) specific heat for ABS, PLA, PU, and C-PLA.

T_g and C_p are shown in Figure 5a and Figure 5b, respectively. T_g and C_p were calculated from the raw DSC data reported in Reference 14. Since PU is elastomeric, its bulk T_g is -45°C. Therefore, the T_g value for FDM PU was not measured using the temperature range of the DSC technique employed in this study. For PLA, ABS and C-PLA FDM parts, the measured T_gs were very close to the bulk values. In addition, C_p values for FDM ABS and PU deviated by 5%, while PLA deviated by ~16%. From these results, we conclude that the T_g and C_p values of FDM parts are isotropic, and are not strongly affected by the FDM process. Therefore, the bulk T_g and C_p values, when available, may be used directly in a material model without further testing.

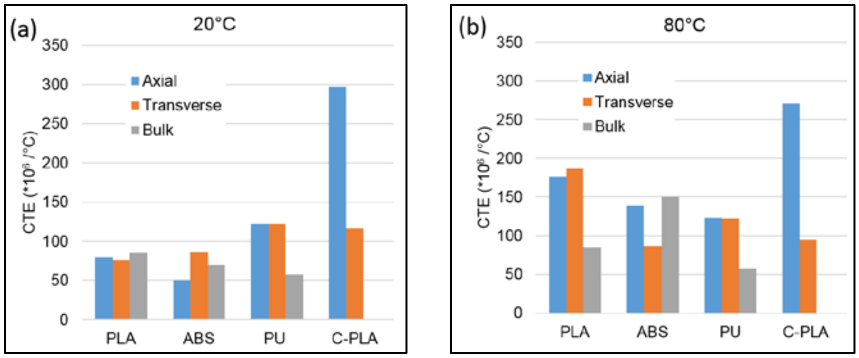

Figure 6. CTEs of PLA, ABS, PU, and C-PLA at (a) 20°C and (b) 80°C.

CTE values are reported at 20°C (a) and at 80°C (Figure 6b). CTE values were calculated from the raw thermal expansion data reported in Reference 14. For PU, the glass transition temperature was never exceeded, so both CTE values are identical. PLA and PU exhibit isotropic thermal expansion behavior, and could be modelled as such. At both of these temperatures, strong anisotropic expansion is shown in the C-PLA sample, where the axial CTE is more than 65% larger than the transverse CTE at both temperatures. ABS also demonstrates anisotropic CTEs. At 20°C, transverse CTE is over 40% larger, however at 80°C, axial CTE is over 37% larger. The nature of these inconsistent CTE values is currently under investigation. Due to these responses, anisotropic thermal expansion modelling is required for both C-PLA and ABS.

Development of a transversely isotropic material model

To illustrate the effects of material anisotropy on the mechanical part response of PLA under a tensile load, a transversely isotropic model was developed and solved in ANSYS. In this model, the properties in the transverse directions (XY plane in Figure 1b) are equal and substantially different than those in axial direction (Z-direction in Figure 1b). Tensile properties were assumed to be identical to compressive properties shown in Figure 2 through Figure 4. Density was taken from bulk literature values and shear modulus was assumed to be half of the elastic modulus.

The response of a contour-free PLA tensile specimen under due to 2.5 kN axial tensile load was modelled. Two anisotropic cases were compared, where (i) the transverse and (ii) the axial properties were oriented in the load direction. For each case, the complementary property was applied to directions normal to the load. The isotropic case was also compared, where (iii) the bulk properties of PLA were used.

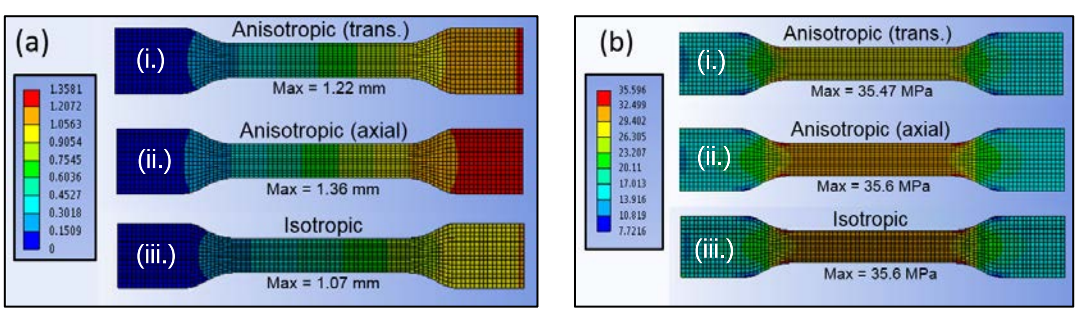

Figure 7. Modelled (a) deflection and (b) stress in specimens due to a 2.5 kN tensile load.

Results shown in Figure 7a demonstrate that maximum deflection is 11.5% larger in the axial direction compared to the tensile direction. These values are between 14% and 27% larger than the maximum deflection predicted using bulk PLA properties in an isotropic material model. Maximum stresses are nearly identical between the isotropic and anisotropic models, however tensile stress in the center of the sample is ~15% higher in the isotropic model (Figure 7b). These results confirm that anisotropy has a significantly affects the mechanical response of FDM parts. Such a model may be further expanded to include the effects of unidirectional contours on the overall part response. The necessity of using an anisotropic model compared to a fully isotropic model, however, will depend on the required accuracy of the model output.

CONCLUSIONS AND FUTURE WORK

In this work, anisotropic behavior was measured in PLA, ABS, PU, and C-PLA parts fabricated using FDM. PLA, ABS, and PU all show greater than 10% anisotropy between the axial and transverse directions for most compressive properties, whereas C-PLA is isotropic. ABS and C-PLA, however, have CTE anisotropy between 35 and 65%, while PLA and PU are isotropic. The T_g and C_p of FDM parts were found to be determined by the bulk values of the material, itself.

These isotropic vs. anisotropic assignments for compressive and CTE properties will largely depend on the required accuracy of the material model. In strongly anisotropic FDM materials, a two-component transversely isotropic material model may be employed, where the contours and infill are characterized separately and modelled in unison. Such results may be applied to improve and develop material models in order to more accurately predict the thermal and mechanical response of FDM parts for functional applications.

REFERENCES

1. Sbriglia, L. R., A. M. Baker, J. M. Thompson, R. V. Morgan, A. J. Wachtor, J. D. Bernardin. 2016. *Topics in Modal Analysis and Testing*, 10:205-214.
2. Rumley-Ouellette, B. J., J. Wahry, A. M. Baker, J. D. Bernardin, M. D. Todd, A. N. Marchi, *11th International Workshop on Structural Health Monitoring*, Stanford, CA, U.S.A., September 2017.
3. Wahry, J., B. J. Rumley-Ouellette, A. M. Baker, J. D. Bernardin, M. D. Todd, A. N. Marchi. *11th International Workshop on Structural Health Monitoring*, Stanford, CA, U.S.A., September 2017.
4. Bikas, H., P. Stavropoulos, G. Chryssolouris. 2016. *Int. J. Adv. Manuf. Technol.*, 83:389–405.
5. Bagsik, A., V. Schöppner, E. Klemp. *14th International Scientific Conference on Polymeric Materials*, Halle (Saale), Germany, September 2010.
6. Bhate, D. "Modeling FDM Structure & Properties: The Key to Enabling Functional Part Production," Phoenix Analysis and Design Technologies Webinar, June 2016.
7. Bagsik, A., V. Schöppner, E. Klemp. *69th Annual Technical Conference of the Society of Plastics Engineers*, Boston, MA, U.S.A., May 2011.
8. OptiMatter Material Database, Retrieved from https://www.optimatter.com.
9. Tymrak, B. M., M. Kreiger, J. M. Pearce. 2014. *Mater. Des.*, 58:242-246.
10. Casavola, C., A. Cazzato, V. Moramarco, C. Pappalettere. 2016. *Mater. Des.*, 90:453-458.
11. Stratasys ABS-M30 Material Datasheet, Retrieved from http://www.stratasys.com.
12. NinjaTek PLA Material Datasheet, Retrieved from http://www.ninjatek.com.
13. Faridmehr, I., M. H. Osman, A. B. Adnan, A. F. Nejad, R. Hodjati, M. Azimi. 2014. *Am. J. Civ. Eng. Archit.*, 2(1):53-59.
14. Dataset retrieved from dx.doi.org/10.13140/RG.2.2.34659.35362.